

Isothermal–Isobaric Molecular Dynamics Simulations of 1,3,5,7-Tetranitro-1,3,5,7-tetraazacyclooctane (HMX) Crystals

Dan C. Sorescu,^{†,‡} Betsy M. Rice,^{*,§} and Donald L. Thompson^{*,†}

Department of Chemistry, Oklahoma State University, Stillwater, Oklahoma 74078, and
The U. S. Army Research Laboratory, Aberdeen Proving Ground, Maryland 21005

Received: March 27, 1998; In Final Form: June 3, 1998

Isothermal–isobaric molecular dynamics (NPT-MD) simulations of the β , α , and δ phases of crystalline 1,3,5,7-tetranitro-1,3,5,7-tetraazacyclooctane (HMX) were performed over the temperature range 4.2–553 K and 1 atm. The Buckingham repulsion–dispersion intermolecular potential developed for hexahydro-1,3,5-trinitro-1,3,5-s-triazine (RDX) (*J. Phys. Chem.* **1997**, B101, 798) with electrostatic charges determined by ab initio calculations was used to describe the HMX crystal phases. The predicted space group symmetries and structural parameters for the three phases of HMX are in close agreement with experimental values.

We recently reported¹ the degree of transferability of an intermolecular potential that was parameterized to describe the α -form of the hexahydro-1,3,5-s-triazine (RDX) crystal² to the new explosive 2,4,6,8,10,12-hexanitrohexaazaisowurtzitane (HNIW), a polycyclic nitramine that resembles two bridged RDX molecules. Molecular packing (MP) and isothermal–isobaric molecular dynamics (NPT-MD) simulations showed good agreement between the predicted geometrical parameters and the experimental values for the ϵ , β , and γ phases of HNIW.¹ Additionally, the calculations indicate a stability ranking order $\epsilon > \beta > \gamma$, in agreement with experimental measurements.³ An extension of these investigations is presented in this work, in which we determine the extent to which this potential describes the 1,3,5,7-tetranitro-1,3,5,7-tetraazacyclooctane (HMX) crystals, one of the most widely used ingredients in various propellants and explosives.⁴ In particular, we have investigated the role of thermal effects on the structural parameters of different phases of this crystal, namely, α , β , and δ (see Figure 1).

Crystalline HMX can exist in four polymorphic phases, known as the α , β , γ , and δ forms. The stable form at room temperature is β -HMX. It has a monoclinic structure with $P21/n$ symmetry^{5,6} or alternatively $P21/c$,⁷ and with $Z = 2$ molecules per unit cell. The α -HMX crystal structure was reported to be stable in the temperature range 103–162 °C.⁸ This phase crystallizes in the orthorhombic $Fdd2$ symmetry and has eight molecules in the unit cell.⁹ The δ -polymorph is stable above 160 °C up to the melting point (280 °C).⁹ The crystals of this phase are hexagonal with space group $P6_1$ and $Z = 6$ molecules per unit cell.¹⁰ The conformations of the β - and α -HMX molecules are quite different; the β -HMX has a center of symmetry, while the molecules in α -HMX have a basket-like shape with 2-fold symmetry (see Figure 1). The shape of the molecules in the δ phase is similar to that of the α -polymorph with approximately 2-fold symmetry about an axis perpendicular to the ring plane through the center of the ring. The remaining polymorph of HMX, γ , is a hydrate. This phase is metastable

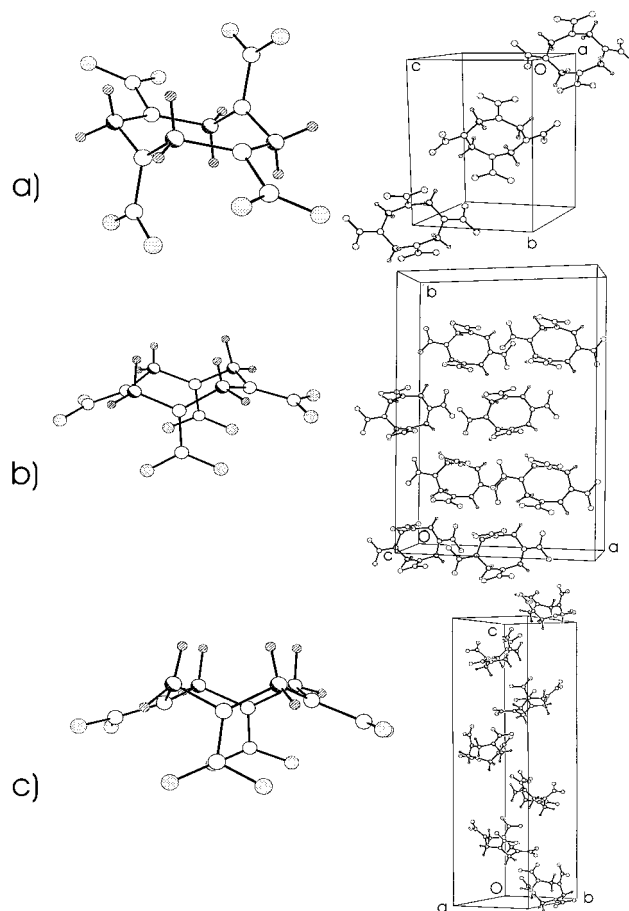


Figure 1. Molecular and crystal configurations of HMX in phases (a) β ; (b) α ; (c) δ .

for all temperatures at atmospheric pressure. Crystals of γ -HMX have Pn symmetry with $Z = 2$ molecules per unit cell.¹¹ We have not considered this hydrated phase in this study.

We have performed molecular packing calculations for the α , β , and δ phases of HMX, under the assumption of the rigid molecules, the results of which are included in a forthcoming study that determines the extent of transferability of the RDX

[†] Oklahoma State University.

[‡] Current mailing address: Department of Chemistry, University of Pittsburgh, Pittsburgh, PA 15260.

[§] U.S. Army Research Laboratory.

TABLE 1: Predicted Thermal Expansion Coefficients (χ) and Lattice Parameters as Functions of Temperature

T (K)	a (Å)	b (Å)	c (Å)	α (deg)	β (deg)	γ (deg)	volume (Å ³)
β-HMX							
MP ^a	6.4756	10.8316	7.3733	90.00	99.91	90.00	509.45
4.20	6.4765 \pm 0.0107	10.8335 \pm 0.0307	7.3740 \pm 0.0190	90.00 \pm 0.01	99.91 \pm 0.13	90.00 \pm 0.04	509.65 \pm 1.35
100.00	6.4922 \pm 0.0233	10.8709 \pm 0.0449	7.3833 \pm 0.0405	89.99 \pm 0.15	99.96 \pm 0.30	90.00 \pm 0.19	513.23 \pm 2.09
200.00	6.5106 \pm 0.0176	10.9124 \pm 0.0335	7.3934 \pm 0.0266	90.00 \pm 0.19	99.99 \pm 0.28	89.98 \pm 0.24	517.28 \pm 2.05
273.15	6.5242 \pm 0.0238	10.9525 \pm 0.0373	7.3982 \pm 0.0296	90.01 \pm 0.29	100.01 \pm 0.27	89.96 \pm 0.32	520.56 \pm 2.22
300.00	6.5257 \pm 0.0250	10.9580 \pm 0.0389	7.4059 \pm 0.0298	90.00 \pm 0.30	100.07 \pm 0.28	90.00 \pm 0.29	521.39 \pm 2.11
350.00	6.5348 \pm 0.0282	10.9792 \pm 0.0478	7.4127 \pm 0.0373	90.01 \pm 0.28	100.07 \pm 0.32	89.99 \pm 0.26	523.62 \pm 2.76
exptl ^b	6.5347	11.0296	7.3549	90.00	102.69	90.00	517.16
χ^c	2.4458	4.0820	1.7752				8.2416
α-HMX							
MP ^a	14.9760	23.6617	6.0191	90.00	90.00	90.00	2132.91
376.00	15.1232 \pm 0.0531	23.9433 \pm 0.0750	6.0690 \pm 0.0221	89.97 \pm 0.51	89.97 \pm 0.61	90.12 \pm 1.23	2196.75 \pm 9.71
400.00	15.1427 \pm 0.0651	23.9468 \pm 0.0839	6.0720 \pm 0.0248	89.98 \pm 0.57	90.06 \pm 0.81	90.07 \pm 1.06	2201.70 \pm 11.85
435.00	15.1556 \pm 0.0625	23.9913 \pm 0.0786	6.0750 \pm 0.0286	89.99 \pm 0.62	89.97 \pm 0.53	90.30 \pm 1.10	2207.08 \pm 11.27
450.00	15.1601 \pm 0.0554	24.0116 \pm 0.0874	6.0782 \pm 0.0242	90.02 \pm 0.52	89.95 \pm 0.78	90.00 \pm 1.43	2211.57 \pm 12.47
exptl ^b	15.1400	23.8900	5.9130	90.00	90.00	90.00	2138.70
γ^c	3.2316	4.1170	1.9322				8.9871
δ-HMX							
MP ^a	7.6681	7.6681	33.5947	90.00	90.00	120.00	1710.71
433.00	7.7802 \pm 0.0306	7.7762 \pm 0.0290	34.0047 \pm 0.1315	89.98 \pm 0.30	90.01 \pm 0.32	119.97 \pm 0.30	1781.96 \pm 7.36
475.00	7.7818 \pm 0.0313	7.7818 \pm 0.0372	34.0623 \pm 0.1343	90.01 \pm 0.34	90.00 \pm 0.34	120.00 \pm 0.38	1786.10 \pm 7.62
500.00	7.8000 \pm 0.0406	7.8015 \pm 0.0397	34.1202 \pm 0.1896	90.00 \pm 0.35	90.03 \pm 0.35	120.06 \pm 0.39	1798.09 \pm 8.17
553.00	7.8155 \pm 0.0378	7.8104 \pm 0.0328	34.1954 \pm 0.1643	90.03 \pm 0.40	89.98 \pm 0.40	119.98 \pm 0.37	1804.31 \pm 8.38
exptl ^b	7.7110	7.7110	32.5530	90.00	90.00	120.00	1676.27
χ^c	4.1388	4.0023	4.8635				11.7040

^a MP: molecular packing; taken from Sorescu et al., ref 12. ^b The data are for $T = 295$ K. α , ref 9; β , ref 6; δ , ref 10. ^c Units: linear expansion coefficients are in 10^{-5} K⁻¹; volume expansion coefficient 10^{-5} K⁻¹.

potential to 30 nitramine crystals.¹² The general good agreement found between the predicted and experimental crystallographic parameters for these crystals indicates that the Buckingham potentials developed for RDX can be used as a general nitramine potential. This conclusion is also reported by the calculated lattice energies. For example, the molecular packing lattice energies for the β , α , and δ phases of HMX crystals are -180.23 , -179.15 , and -168.24 kJ/mol, respectively.¹² These values support the polymorph stability ranking $\beta > \alpha > \delta$ found experimentally by McCrone.¹³ Also, the lattice energies are in good agreement with the values determined from the experimental heats of sublimation. Indeed, the heats of sublimations for β and δ phases are respectively 175.2 kJ/mol^{14a} and 161.9 kJ/mol,^{14b} which lead¹⁵ to values of -180.29 and -166.94 kJ/mol for the corresponding lattice energies. We are not aware of a value for the experimental heat of sublimation of the α phase.

Besides the absolute values of the lattice energies, it is important to provide the contributions of the individual potential terms. Specifically, the particular values of dispersion, repulsion, and Coulombic terms for the β , α , and δ phases are, respectively, $E_{\text{disp}} = -219.62$ kJ/mol, $E_{\text{rep}} = 105.31$ kJ/mol, $E_{\text{Coul}} = -65.92$ kJ/mol; $E_{\text{disp}} = -198.01$ kJ/mol, $E_{\text{rep}} = 93.29$ kJ/mol, $E_{\text{Coul}} = -74.44$ kJ/mol; and $E_{\text{disp}} = -174.60$ kJ/mol, $E_{\text{rep}} = 78.89$ kJ/mol, $E_{\text{Coul}} = -72.52$ kJ/mol. These results indicate that in the case of HMX crystals the lattice energies are sensitive to both the repulsion and dispersion as well as the electrostatic terms.

The quality of the results predicted by the present intermolecular potential represents an improvement relative to previous theoretical work. For example, in a similar attempt to predict the structure and energies of HMX polymorphs on the basis of packing calculations, Dzyabchenko et al.¹⁶ have obtained a reasonable agreement with the X-ray structural data, but the computed lattice energies were not accurate enough to predict the observed heats of sublimation and the trend of polymorph

stabilities. In the case of our potential, both lattice parameters and the lattice energies and the polymorph stability ranking have been found to agree with experimental results.

In the present study we investigate the temperature effects on the crystallographic structural parameters of HMX crystals through NPT-MD simulations. The use of this method represents a more realistic approach to predict the structural lattice parameters when compared with the static molecular packing calculations. At the same time, the use of the rigid molecular model in the present calculations imposes some limitations, particularly related to the energy transfer in molecules.¹⁷ However, for the temperature and pressure range used in this study, the intramolecular energetic effects have only a small role on the equilibrium properties of the crystals.

The functional form of the interaction potential used, which includes an explicit description of the electrostatic interactions, and a description of the simulation method have been described previously.^{1,2} It is assumed that the dispersive and repulsive terms of the RDX potential are transferable to the HMX crystals. However, the set of electrostatic charges assigned to the atoms in the HMX molecule were calculated for each particular phase by fitting atom-centered partial charges to a quantum mechanically derived electrostatic potential. The experimental molecular conformations were used in these calculations, and the partial charges were fitted to the electrostatic potential calculated at MP2/6-31G** level. The MD simulation cell consists of a box containing 24 ($4 \times 2 \times 3$), 8 ($2 \times 1 \times 4$), and 16 ($4 \times 4 \times 1$) crystallographic unit cells for the phases β , α , and δ , respectively. The corresponding cutoff distances were $R_{\text{cut}} = 10.0$, 10.0 , and 11.0 Å, respectively.

The crystal structure information resulting from NPT-MD simulations at atmospheric pressure and various temperatures is given in Table 1. Lattice dimensions for β -HMX obtained at $T = 4.2$ K are in very close agreement with those determined in the molecular packing calculations with symmetry constraints. This is expected since the thermal effects at this temperature

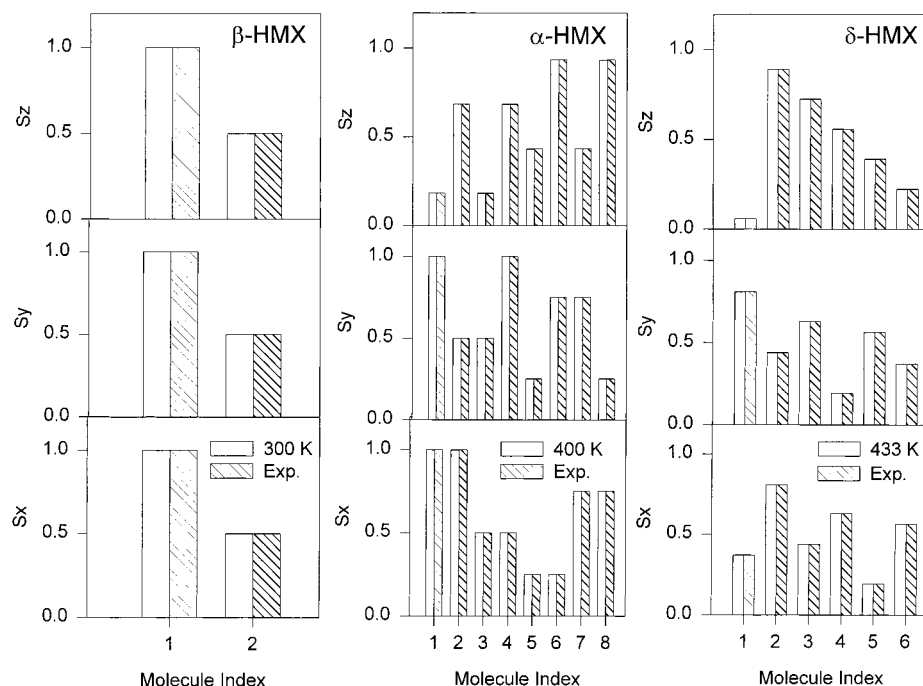


Figure 2. Comparison of the time-averaged center-of-mass-fractional positions with experiment for β -, α -, and δ -HMX. These time averages for each molecule in the unit cell were averaged over the 24, 8, and 16 unit cells in the simulation box for, respectively, the β -, α -, and δ -HMX phases.

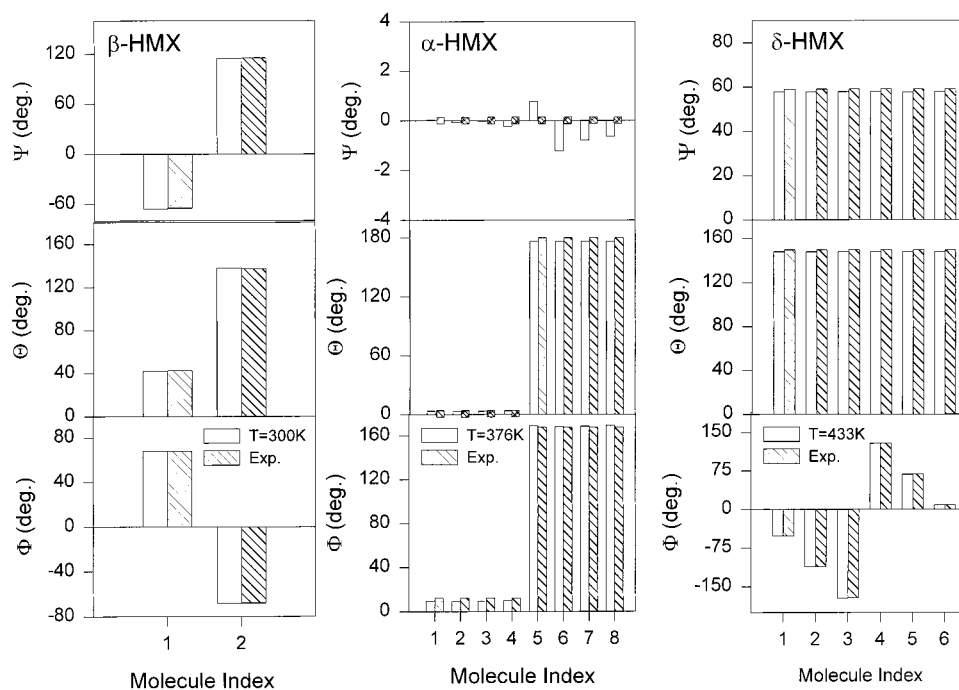


Figure 3. Comparison of the time-averaged Euler angles (X-convention¹⁸) with experiment for β -, α -, and δ -HMX. These time averages for each molecule in the unit cell were averaged over the 24, 8, and 16 unit cells in the simulation box for, respectively, the β -, α -, and δ -HMX phases. In the case of the Θ and Ψ angles for α -HMX, the double-crossed squares indicate an equilibrium value of 0° .

should be minimal and the results should be close to the values corresponding to the potential energy minimum. The average lattice dimensions a , b , c of the β -phase agree very well with the experimental values at 300 K, the differences being 0.13%, 0.65%, and 0.69%, respectively. The corresponding deviations for the α and δ phases, at 376 K, are 0.11%, 0.22%, and 2.6%; and 0.89%, 0.83%, and 4.4% at 433 K. In addition, the angles of the unit cell remain close to the experimental values for all three phases, with a maximum difference of 2.5% for the β angle of the β -HMX. However, it should be noted that in the case of

α - and δ -HMX, the experimental crystallographic results^{9,10} are for $T = 295$ K despite the fact that this temperature is outside the stability range of these two phases.

Figures 2 and 3 compare the results of the average mass-center fractionals and Euler angles for each molecule in the unit cell with the corresponding experimental data for all three phases. In the case of β phase, there are no significant displacements of the molecular mass-centers or increase of the degree of rotational disorder. Similar results are obtained for the α and δ phases. For example, the largest difference between

experiment and predictions of molecular orientation occurs for the Euler angle Θ for α -HMX; the predicted average value is 3.8° larger than the experimental value.

The temperature dependence of the cell edges is used to extract the linear and the volume thermal expansion coefficients. These values are given in Table 1. For β -HMX, two values ($3.96 \times 10^{-5} \text{ K}^{-1}$ and $5.04 \times 10^{-5} \text{ K}^{-1}$) for the linear expansion coefficients have been reported in the temperature range 219–347 K.¹⁹ The measured linear expansion coefficients are in relatively good agreement with the values predicted by our potential, particularly for lattice edges a and b . The expansion coefficient for c is significantly smaller than the experimental values. The value $16.25 \times 10^{-5} \text{ K}^{-1}$ for the volume expansion coefficient has been reported for the temperature interval 243–343 K;¹⁴ this is a factor of 2 larger than our predictions. No experimental values were available for the α and δ phases for comparison. The calculated expansion coefficients for the α and β phases are close in value, and the differences in the linear expansion coefficients for the different cell edges in both polymorphs indicate anisotropic thermal behavior. Conversely, the three linear expansion coefficients for δ -HMX are almost equal, indicating an isotropic expansion.

The success of this potential in describing these three phases of the HMX crystal at moderate temperatures and low pressure provides incentive to further investigate the transferability of this model to other nitramines. The results of such molecular packing studies of 30 nitramine crystals show that this potential is transferable.¹²

Acknowledgment. This work was supported by the Strategic Environmental Research and Development Program (SERDP), Project PP-695. D.L.T. gratefully acknowledges support for the U.S. Army Research Office under Grant DAAG55-98-1-0089.

References and Notes

(1) Sorescu, D. C.; Rice, B. M.; Thompson, D. L. *J. Phys. Chem.* **1998**, *B102*, 948.

(2) Sorescu, D. C.; Rice, B. M.; Thompson, D. L. *J. Phys. Chem.* **1997**, *B101*, 798.

(3) Russell, T. P.; Miller, P. J.; Piermarini, G. J.; Block, S.; Gilardi, R.; George, C.; AD-CO48 931 (92-0134), p 155, Apr 91, CPIA Abstract No. 92, 0149. ADD604 542. C-D, Chemical Propulsion Information Agency, 10630 Little Patuxent Parkway, Suite 202, Columbia, MD 21044-3200.

(4) Rogers, J. T. *Physical and Chemical Properties of RDX and HMX*; Report HDC-20-P-26-SER-B, Holston Defense Corporation, Kingsport, TN, Aug. 1962; CPIA Abstract 73-1016, AD 904-410L, U-B.

(5) Eiland, P. R.; Pepinsky, R. Z. *Kristallogr.* **1995**, *106*, 273.

(6) Kohno, Y.; Maekawa, K.; Azuma, N.; Tsuchioka, T.; Hashizume, T.; Imamura, A. *Kogyo Kagaku* **1992**, *53*, 227 (in Japanese).

(7) Choi, C. S.; Boutin, H. P. *Acta Crystallogr.* **1970**, *B26*, 1235.

(8) Cady, H. H.; Smith, L. C. Los Alamos Scientific Laboratory Report No. LAMS-2652; Los Alamos Laboratory: 1961.

(9) Cady, H. H.; Larson, A. C.; Cromer, D. T. *Acta Crystallogr.* **1963**, *16*, 617 (Y coordinate of N₁ given as 0.0599 in table 2 should be negative).

(10) Cobbleddick, R. E.; Small, R. W. H. *Acta Crystallogr.* **1974**, *B30*, 1918.

(11) Main, P.; Cobbleddick, R. E.; Small, R. W. H. *Acta Crystallogr.* **1985**, *C41*, 1351.

(12) Sorescu, D. C.; Rice, B. M.; Thompson, D. L. *J. Phys. Chem.* Submitted.

(13) McCrone, W. C. In *Physics and Chemistry of the Organic Solid State*; Fox, D., Labes, M. M., Weissberger, A., Eds.; Wiley: New York, 1965; Vol. II, pp 726–766.

(14) (a) Rosen, J. M.; Dickinson, C. J. *Chem. Eng. Data* **1969**, *14*, 120. (b) Taylor, J. W.; Crookes, R. J. *J. Chem. Soc., Faraday Trans. 1* **1976**, *72*, 723.

(15) *Fundamentals of Crystallography*; Giacovazzo, C., Ed.; Oxford University Press: New York, 1992.

(16) Dzyabchenko, A. V.; Pivina, T. S.; Arnautova, E. A. *J. Mol. Struct.* **1996**, *378*, 67.

(17) Kohno, Y.; Ueda, K.; Imamura, A. *J. Phys. Chem.* **1996**, *100*, 4701.

(18) Goldstein, H. *Classical Mechanics*; Addison-Wesley: Reading, MA, 1980.

(19) Dobratz, B. M. In *Properties of Chemical Explosives and Explosive Simulants*; Report No. UCRL-52997; Lawrence Livermore Laboratory: Livermore, CA, March 1981; pp 19-55 to 19-56, U-A.